

Improvement of Privacy Prevented Person Tracking System using Artificial Fiber Pattern

Hiroki Urakawa, Kitahiro Kaneda and Keiichi Iwamura
Tokyo University of Science 6-3-1 Niijuku, katusika-ku Tokyo, 125-8585, Japan

Keywords: Data Hiding, Surveillance Camera, Deep Learning, Artificial Fiber Pattern, Object Detection, Image Reconstruction.

Abstract: Owing to the low equipment cost, the number of surveillance cameras installed has increased significantly; however, most of them are not being used effectively. These cameras can be used for various purposes, such as marketing, if behavior tracking is possible from the obtained images. Previously, we proposed a method of tracking by embedding information in "Artificial Fiber Pattern." However, the body shape of the wearer and wrinkles of the clothes affect the accuracy of the results. To overcome this drawback, in this study, we combined PIFu HD, a technology that generates a full three-dimensional model from a single image of a person, with the modeling and calculation of the body shape of the subject to verify the conditions under which the body shape of the wearer and wrinkles in the clothes affect the accuracy. Consequently, we achieved precision improvement by removing data that met unsuitable conditions.

1 INTRODUCTION

Recently, the price of cameras has dropped, and consequently, countless surveillance cameras have been installed at various locations in cities. An enormous amount of data is obtained from surveillance cameras, and in the era of information technology, it is expected to have a great value beyond the original purpose of installation, which includes "crime prevention" and "criminal investigation".

Surveillance cameras, which are in constant operation at various locations, are effective devices for use in human flow analysis. The purpose of this study is to use the data obtained from surveillance cameras effectively for "crime prevention" and "trend investigation for marketing, events, advertisement, etc.

In our previous research, (Kaneda, et al., 2008), and (K. Kaneda, et al., 2010), behavioral tracking using surveillance cameras was performed by embedding information in specific patterns in clothing. Existing methods for embedding information in patterns include QR codes and barcodes; however, these methods are visually uncomfortable and are not suitable for clothing that requires a good design. Therefore, we use "Artificial

Fiber Pattern," which is less visually distracting and more resistant to noise. In addition, by automating the system using general object detection technology based on deep learning, a human-dynamics monitoring system can be realized that obtains time and location information with high accuracy and low cost. However, as the patterns are embedded in clothes, the patterned area is deformed by the wearer's body shape and wrinkles in the clothes, thus significantly degrading the accuracy of the system. The advantage of the Artificial Fiber Pattern over conventional person tracking methods (e.g., tracking by face recognition) is its superior privacy protection. While tracking by face recognition requires the system to retain the privacy information of the individual's face, the Artificial Fiber Pattern does not.

In this study, we modeled the three-dimensional (3D) shape of the wearer using machine learning, estimated the deformation of the embedded area of the pattern, and verified whether the detection accuracy can be improved by rejecting problematic areas and frames in comparison with the conditions that reduce the accuracy.

2 CONVENTIONAL RESEARCH

2.1 Background

Numerous studies have been conducted on the embedding of information in printed materials, which can be categorized into two main types, visible and invisible. The visible method is represented by QR codes and barcodes, whereas the invisible method is represented by digital watermarks. The visible method has the advantage of a large and stable amount of information that can be embedded; however, it has the disadvantage of a large subjective sense of discomfort and a low degree of freedom in design. Conversely, the invisible method has the advantage of less subjective discomfort but has the disadvantage of limited embedding content and small embedding capacity. There is a trade-off between discomfort and information volume, and no embedding method satisfies both.

Therefore, we devised a method of embedding information that allows us to recognize changes in the content and has less subjective discomfort; we defined it as an artificial fiber pattern. The information was embedded by updating the frequency domain based on the pattern originally contained in the embedding target. Consequently, there is less subjective discomfort even though the image quality is improved compared to conventional artificial patterns, and the effects of geometric deformation, printing resistance, and paper shape change due to low visibility are decreased. Specifically, as shown in Fig. 1, the embedded frequency components are varied to the extent that the change in content can be recognized, but with less subjective discomfort.

At the time of extraction, the embedded pattern information obtained by the camera or scanner was compared with the neighboring embedded information using an intensity ratio and a threshold was used. Thus, the intensity ratio is 1 if the adjacent embedded information and the target artificial fiber pattern are the same, and it is far from 1 if they are different, as shown in Fig. 2. The information was extracted by determining the intensity ratio with an appropriately set threshold. This information is presented in the references of (Inui et al., 2019, Tomita et al., 2017, Iwamura et al., 2017, Noguchi et al., 2018, Tomita et al.2018, Urakawa et al., 2021)

2.2 Artificial Fiber Pattern using Designs

In the literature (K. Kaneda, et al., 2008, K. Kaneda, et al., 2010) artificial fiber patterns are generated by

coloring various paper patterns in cyan, magenta, and yellow to embed information in everyday patterns (Fig. 3 and 4). The amount of extracted information is (11 bits embedded in a sheet of A4 size paper) × (10 shots) = 110 bits.

2.3 Embedding the Man-Made Fiber Pattern into the Fabric

Extraction rate in a previous study as adopted as the prototype pattern, and the artificial fiber pattern was generated using the procedure described in Section 2 (Fig. 3). The generated artificial fiber pattern was converted to cyan and printed on "3M Japan Corporation Cloth Prefabricated Type Glue-less" for the experiment. An example of the processed image after photographing the printed artificial fiber pattern is shown in Fig. 5.

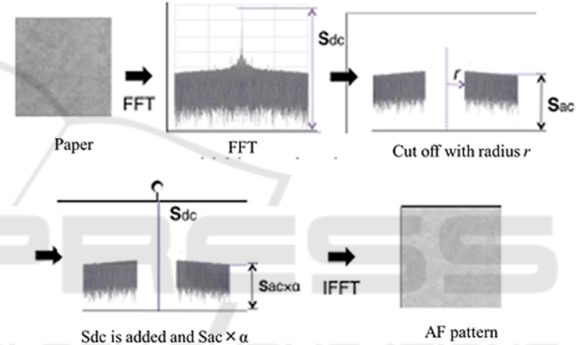


Figure 1: Procedure for generating Artificial Fiber Pattern.

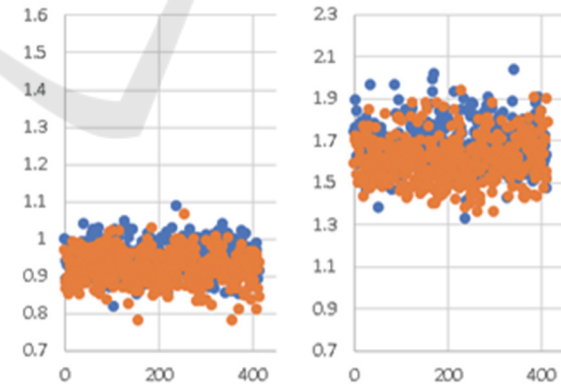


Figure 2: Distribution of intensity values (Vertical axis: intensity ratio Horizontal axis: frame number) Left: Different pattern Right: Same pattern.



Figure 3: Colorized patterns.

In the experiment, we used a Canon Web View Livescope VB-H43 (Full HD video recording: 1920×1080) as a surveillance camera to capture the man-made fiber pattern (11 bits) from a distance of 1.5 m and verified the extraction accuracy for 54 consecutive frames.

Consequently, 86.3% of the information was obtained, and 100% of the extraction rate was obtained for frames with large edge values. The edge values of each image and the number of errors at that time are summarized in Table 1.

2.4 YOLOv5

Because processing speed is an important factor in the human motion monitoring system that we aim to develop, we used You Only Look Once (YOLO), a fast general object detection method, to identify clothes and extract pattern regions of artificial fibers. In previous research, YOLO version 3 (YOLOv3) was used for clothing identification and the extraction of difficult-to-see pattern regions. In this study, we upgraded to YOLOv5, which is a newer version of YOLOv3.

Fig. 6 shows that YOLOv5 has higher accuracy than YOLOv3 and other methods. This image was sourced from references (Huang et al.,2021) and (Bochkovskiy et al.,2020). In order to achieve real-time monitoring, high-speed processing that consistently exceeds the number of recorded frames is necessary. In this study, YOLOv5 was chosen to achieve both low load and high accuracy.

Fig. 7 shows the flow of the information extraction. First, YOLOv5 detects the pattern regions of clothing and artificial fibers. The extracted man-made fiber pattern area is pre-processed by projection transformation, grayscale transformation, histogram flattening, and color map adjustment and divided into cells. Subsequently, the intensity ratio of the adjacent cells is calculated, and the information extracted from the threshold is recorded on a voting table. The pattern is determined by the majority vote among the voting results of all frames. As depicted in Fig. 7, the value is "0" if the adjacent cells are the same, and "1" if the adjacent cells are different.

3 PROPOSED METHOD

3.1 Overview

In our previous research, we built a person tracking system using surveillance cameras by automating the reading of an artificial fiber pattern in video.

However, when using this system outdoors, its accuracy was strongly affected by the wearer's body shape and movement because the patterns were embedded in clothing.

Therefore, in this study, we improved the system such that the influence of the wearer's body shape and movement is reduced.

To estimate and quantify body shape and movement, we created 3D data using "PIFu HD," a system that can accurately model body shape from still images. We evaluated the data using our method to quantitatively calculate the degree of body shape and wrinkles.

By calculating the numerical values of body shape and wrinkles for multiple videos of people wearing the patterns and comparing the accuracy of the conventional artificial fiber pattern reading system, the range that affects reading accuracy was determined.

Based on these values, if the body shape and wrinkle values were higher than the standard values, the frame could not be judged, thereby reducing the number of false judgments.



Figure 4: Sample of patterns.

3.2 PIFuHD

PIFuHD is the successor to PIFu, a modeling technique that estimates the 3D shape of a person from a single image and enables modeling with a higher resolution than conventional techniques. PIFu is described in detail in (Saito et al.,2019) and (Saito et al.,2020).

Fig. 8 shows the 3D modeling of the actual image of the subject wearing the artificial fiber pattern using the PIFuHD. It can be seen that not only the posture and body shape of the subject but also the wrinkles and other details of the clothing are reproduced.

3.3 Effect of Body Shape and Wrinkles on Accuracy

As mentioned earlier, because the artificial fiber pattern is embedded in clothes, recognition accuracy is degraded by the wearer's body shape and wrinkles.

We examined the impact of these factors on the accuracy. The cloth and the plane connecting the four corners of the artificial fiber pattern in the modeling. This value is known as the deflection value.

3.4 Determination of Body Shape by Modeling Data

Obesity and chest size can be considered as body types that affect the shape of a garment. For a normal body shape, each point on the garment should be on the same plane. However, changes in the shape of the garment according to the body shape will greatly deflect the cloth, and the points will not exist on the same plane.

Therefore, we quantified the extent to which the cloth was deflected depending on the body shape by measuring the average distance between each point of the cloth, we can determine the distance between the cloth and the plane. The amount of wane was quantified by the shape of the body. We call this the deflection value.

3.4.1 Method to Determine Wrinkles

Unlike the change due to body shape, the change in position due to the presence of wrinkles is minor; therefore, it is difficult to make a judgment based on the coordinates of each point on the modeling data.

In this study, the curvature of each point on the modeling data was calculated using the Gaussian curvature. Wrinkles were determined by calculating the curvature of each point on the modeling data using Gaussian curvature.

3.4.2 Gaussian Curvature

An example of a surface at an arbitrary point Q is shown in Fig. 9. This image is sourced from (Okaniwa, Maekawa 2010). The curvature at point Q of the intersection curve between the normal plane and the surface consisting of the unit normal vector N and unit tangent vector T is called the normal curvature. Because the unit tangent vector T can be drawn countless times, normal curvature also exists countless times. The smallest is called the minimum principal curvature, and the largest is called the maximum principal curvature; the product of these two is called the Gaussian curvature.

The larger the absolute value of the Gaussian curvature, the more curved is the surface at that point.

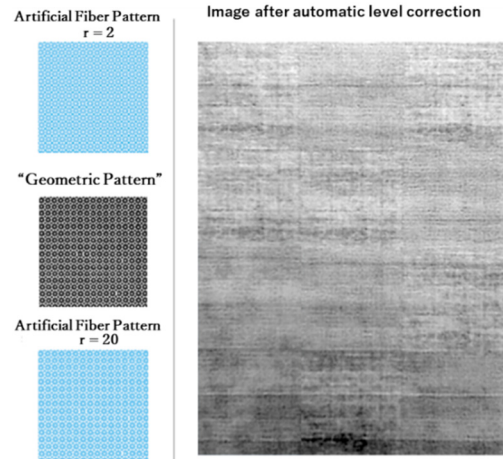


Figure 5: Image after automatic level correction.

Table 1: Relationship between edge number and error number.

Edge	14000~	13000~	12000~	11000~	10000~	9000~	0~
Error count 0	7	14	17	18	19	19	19
Error count 1	0	3	3	10	12	12	12
Error count 2	0	2	6	8	9	9	9
Error count 3	0	0	0	2	3	3	4
Error count 4	0	0	0	0	0	1	2
Error count 5	0	0	0	0	1	2	3
Error count 6	0	0	0	1	1	1	2
Total number	7	19	26	39	45	47	51
Error rate(%)	0.0	3.3	5.2	8.9	10.1	11.4	13.7

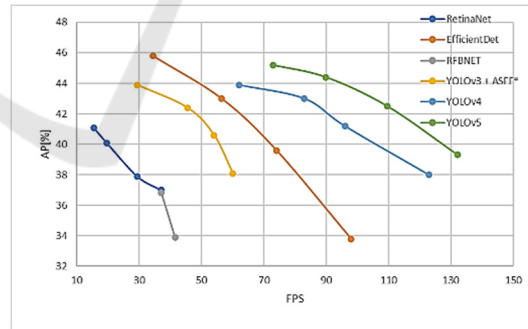


Figure 6: Performance comparison of object detection methods.

3.4.3 Estimation of the Size of Wrinkles

First, by calculating the average of the absolute values of the Gaussian curvature in the region, we can estimate the number of wrinkles in the region. Thereafter, the area of wrinkles in the region can be estimated by counting the number of points where the absolute value of the Gaussian curvature exceeds a certain value.

3.4.4 Determination of Wrinkle Position by Modeling Data

Unlike changes due to body shape, wrinkles are expected to appear locally only on a part of the pattern. If we exclude only the boundary, including the wrinkled pattern, from the judgment, the information contained in the remaining pattern can be extracted accurately.

Fig. 10 shows the layout of the artificial fiber pattern used in this study, which consisted of 12 combinations of patterns in three horizontal rows and four vertical columns. Considering the deflection of the fabric due to the body shape, the first row is 1/18 to 5/18, second row is 7/18 to 11/18, and third row is 13/18 to 17/18; the first row is 1/24 to 5/24, second row is 7/24 to 11/24, third row is 13/24 to 17/24, and 19th row is 19/24. Further, 24 is the third row, 7/24 to 11/24 is the second row, and 19/24 to 23/24 is the fourth row, and the wrinkles in the corresponding area are judged.

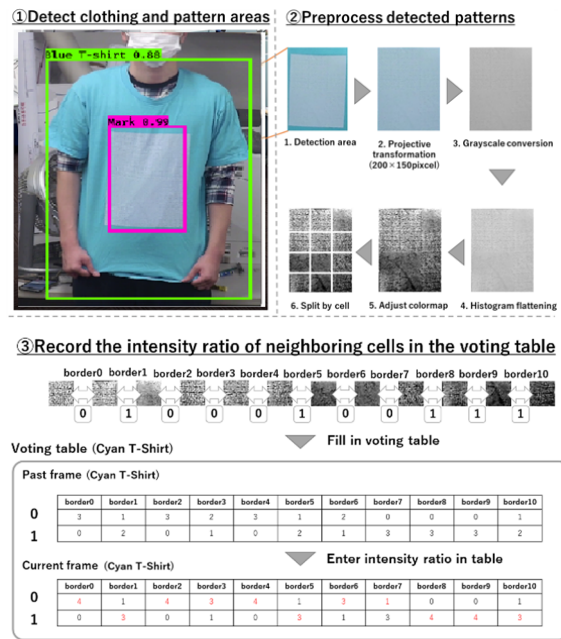


Figure 7: Information extraction flow of the proposed method.

4 EXPERIMENT

4.1 Recording Conditions of the Surveillance Camera

The subjects wore yellow T-shirts embedded with an artificial fiber pattern and stood at a distance of 3 m from a surveillance camera installed in the Iwamura Laboratory.

4.2 Dataset

We prepared 4300 images of three T-shirts (cyan, magenta and yellow) embedded with Artificial Fiber Pattern and trained them on YOLOv5.

4.3 Experimental Environment

- 1) Surveillance camera: Canon Web View Livescope VB-H43 (Full HD video recording: 1920 × 1080)
- 2) Cloth media • Printstar T-shirt Yellow
- 3) Printer for printing • Brother GT-381
- 4) CPU: AMD Ryzen 5900x
- 5) OS: Windows 10 Pro
- 6) GPU: GeForce RTX 3080
- 7) Software used: Python 3.8
- 8) Artificial Fiber Pattern: 2inch square $r=2$ $\alpha=0.65$ • 2inch square $r=20$ $\alpha=0.65$



Figure 8: Modeling by PIFuHD.

4.4 Results

4.4.1 Verification of Appropriate Deflection Values

We reproduced the obese state of the abdomen by placing a cylindrical rolled cushion between the abdomen and T-shirt embedded with the artificial fiber pattern. Four videos were captured for each of the five patterns of the abdominal circumference (73, 85, 95, 105, and 115 cm), and the average deflection values for each pattern and the number of videos that were below 70% in accuracy were compared.

The results are shown in Table 2, which suggests a correlation between abdominal circumference, deflection values, and several misjudgments. In particular, the average deflection value increased

significantly from 85 to 95 cm in the abdominal circumference, resulting in a corresponding increase in the number of misjudgments.

4.4.2 Derivation of Appropriate Gaussian Curvature

As shown in Section 3.3.3, there are two possible criteria for judging wrinkles based on the Gaussian curvature: the total absolute value of the Gaussian curvature and the number of points where the absolute value of the Gaussian curvature exceeds a certain value.

The wrinkles in the clothes were reproduced by inserting a bubble wrap (petit-pouch cushion) in the abdomen while wearing a T-shirt in which an artificial fiber pattern was embedded, and 10 patterns of videos were taken by changing the amount and position of the bubble wrap. However, as the boundaries between different patterns (②, ⑤, ⑧, ⑨, ⑫, ⑬, ⑯, ⑰) are not easily affected by wrinkles, we examined the Gaussian curvature facing each boundary between the same patterns (①, ③, ④, ⑤, ⑧, ⑨, ⑫, ⑬, ⑯, ⑰), which are easily affected by wrinkles (1), (2), (3), (4), (6), (7), (10), (11), (14), and (15). Note that if only one of the two patterns facing each boundary is affected by wrinkles, the Gaussian curvature of the unaffected pattern will be low and that of the affected pattern will be high. The verification results are presented in Table 4.

As shown in Table 4, the Gaussian curvature mean, which does not affect the judgment, is less than 0.07.

Moreover, the range of the Gaussian curvature that can affect the judgment is 0.14 or more. However, this range is too wide, and it is impossible to determine a constant value necessary to estimate the area.

4.4.3 Accuracy Change by Body Shape and Wrinkle Detection

From the data obtained in sections 5.1 and 5.2, the boundary between a person whose average deflection value exceeds 500 and a region containing a pattern whose average Gaussian curvature exceeds 0.1 among all frames is considered as undeterminable.

A total of 15 videos were taken, 5 each wearing a T-shirt embedded with an artificial fiber pattern, holding a cushion in the abdomen, holding a bubble wrapping material and holding nothing in between.

Table 4 shows a comparison of the accuracy between the conventional new methods for the boundary with the lowest accuracy. × means that a

condition that lowers reading accuracy was detected and excluded from the decision. Table 2 shows that only the boundary with the lowest accuracy is avoided.

4.4.4 Discussion and Consideration

The results in Table 4 show that this method was able to reject only those that were not read correctly (3,4,5 with cushion and 3,4,5 with bubble-filled packaging material). It can be said that a kind of error detection function is implemented, a result that leads to improved accuracy. In addition, the accuracy of the two methods with the bubble-wrapping material was better than that of the conventional method. This is because only the problematic area was removed from the judgment, indicating that the local wrinkles could be identified. At present, it is only possible to avoid judging the relevant areas, but further improvement in accuracy is expected by combining it with error-correcting codes.

In addition, the comparison of the area where wrinkles exist, as mentioned in Section 3.3.3, could not be successfully realized. This is because the accuracy was greatly reduced even when there were a small number of wrinkles. However, if we use the absolute value of the Gaussian curvature as an index, we can clearly distinguish the area where the accuracy decreases.

5 SUMMARY

In this study, we modeled the 3D shape of the wearer using PIFuHD, estimated the deformation of the embedded region of the pattern, and verified whether the detection accuracy could be improved by rejecting problematic regions and frames in comparison with the conditions for accuracy loss.

We assumed that the deformation of the embedded area was caused by two factors: "deflection of clothes due to body shape" and "wrinkles". For the former, we attempted to show the degree of deformation by calculating the distance between each point and the plane connecting the four corners of the embedding area, taking advantage of the fact that each point in the model data moved away from the same plane as it was deflected. In the latter case, because the amount of change in the position of each point owing to wrinkles is not very large, it is difficult to measure the degree of wrinkles directly using the coordinates. We attempted to express the degree of wrinkles based on the amount of curvature and the number of points that were bent to a certain degree.

Thus, by calculating the distance between the plane and each point, the deflection of clothes based on the body shape is quantified, and by avoiding judgments of people whose body shape is so deflected that it affects accuracy, we succeeded in reducing misjudgments. Regarding the wrinkle determination using Gaussian curvature, the number of points that were bent more than a certain level was determined from the original number of bent points, and the wrinkles can be identified in which regions of the artificial fiber pattern. Further improvement of the accuracy can be expected by combining with error-correcting codes. In future, we plan to further improve the accuracy by improving the illumination resistance and introduction of error -correcting codes, and to increase the number of bits that can be embedded to include additional information.

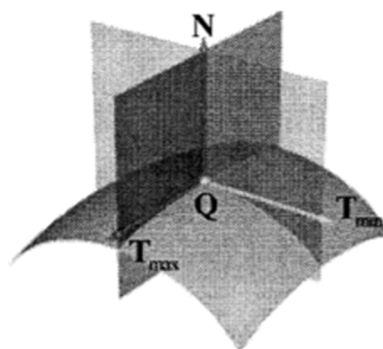


Figure 9: Illustration of Gaussian curvature.

Table 2: Relationship between deflection value and accuracy.

Abdominal circumference [cm]	72	85	95	105	115
Deflection value average	52	243	2174	3821	4592
Number of misjudgments	0	0	2	4	4

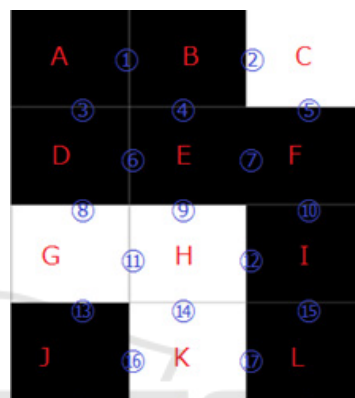


Figure 10: Placement of Artificial Fiber Pattern.

Table 3: Calculation of the appropriate Gaussian curvature.

	Movie Number									
	1	2	3	4	5	6	7	8	9	10
Misjudgment Number	0	0	2	2	3	4	6	10	10	10
Minimum Gaussian curvature when misjudged [%].	×	×	0.15	0.28	0.14	0.24	0.18	0.43	0.49	0.53
Maximum Gaussian curvature when judged correctly [%].	0.03	0.04	0.03	0.03	0.06	×	×	none	none	×

Table 4: Overall accuracy change.

	Normal					With cushion					With Air bubble packing material				
	1	2	3	4	5	1	2	3	4	5	1	2	3	4	5
Previous Method [%]	93	89	86	86	82	84	68	54	22	6.7	78	66	12	0	0
Proposed method [%]	93	89	86	86	82	86	68	×	×	×	78	79	×	×	×

REFERENCE

- Kaneda, K., Hirano, K., Iwamura, K. and Hangai, S (2008) "Information Hiding Method utilizing Low Visible Natural Fiber Pattern for Printed Document," 2008 International Conference on Intelligent Information Hiding and Multimedia Signal Processing, IHMSP2008-IS05-007.
- Kaneda, K. Hirano, K. Iwamura, K. and Hangai, S, (2010) "An Improvement of Robustness against Physical Attacks and Equipment Independence in Information Hiding based on the Artificial Fiber Pattern", WAIS-2010.
- Inui, T. Kaneda, K. Iwamura, K. and Echizen, I., (2014) "Improved proposal of information hiding technology by utilizing an artificial fiber pattern for an augmented reality system, " Proceedings of the Fourth IIEEJ International Workshop on Image Electronics and Visual Computing
- Tomita, W., Kaneda, K., and Iwamura, K., (2017) "Expanding Information Hiding Scheme Using Artificial Fiber (AF) Pattern into Katagami Patterns with a Low-Resolution Web Camera", Proceedings of the Fifth IIEEJ International Workshop on Image Electronics and Visual Computing 2017.
- Iwamura, K. and Kaneda, K. (2017) "Printed Document Protection Using Artificial Fiber Pattern and Its Application" Journal of Printing Science and Technology (JPST), 54-2 p. 103-111
- Noguchi, N., Kaneda, K., and Iwamura, K. (2018) "New approach for embedding secret information into fliber materials", GCCE, October 2018.
- Tomita, W., Noguchi, N., Kaneda, K., Iwamura, K., and Echizen, I. (2018) "Artificial Fiber Pattern ni yoru moyou heno umekomi syuhou no kentou" (A Method for Embedding Information in Patterns Using Artificial Patterns) The institute of Electrical Engineers of Japan 13-4 P435 – 440
- Urakawa, H., Iwamura, K. Kaneda, K. (2021) "Improving a tracking accuracy using Artificial Fiber Patterns by applying a new image processing method" IEICE, vol. 121, no. 29, EMM2021-4, pp. 19-24.
- Huang, X., Wang, X., Lv, W., Bai, X., Long, X., Deng, K., Dang, Q., Han, S., Liu, Q., Hu, X., Yu, D., Ma, Y., Yoshie, O. (2021) "PP-YOLOv2: A Practical Object Detector" arXiv:2104.10419 [cs.CV].
- Bochkovskiy, A., Wang, C. and Liao H. M. (2020) "YOLOv4: Optimal Speed and Accuracy of Object Detection" arXiv:2004.10934 [cs.CV].
- Saito, S., Huang, Z., Natsume, R., Morishima, S., Li, H. and Kanazawa, A. (2019), "PIFu: Pixel-Aligned Implicit Function for High-Resolution Clothed Human Digitization" 2019 IEEE/CVF International Conference on Computer Vision (ICCV).
- Saito, S., Simon, T., Saragih, J. and Joo. H (2020) "PIFuHD: Multi-Level Pixel-Aligned Implicit Function for High-Resolution 3D Human Digitization" CVPR 2020 (Oral Presentation)."
- Okaniwa, S. and Maekawa, S. (2010) "Estimation of Principal Curvatures and Principal Directions for Triangular Meshes" sekkeikougaku sistemubumon kouenkai kouen ronbunshuu 2010.20(0), 3307-1_3307-5_, 2010, The Japan Society of Mechanical Engineers.